

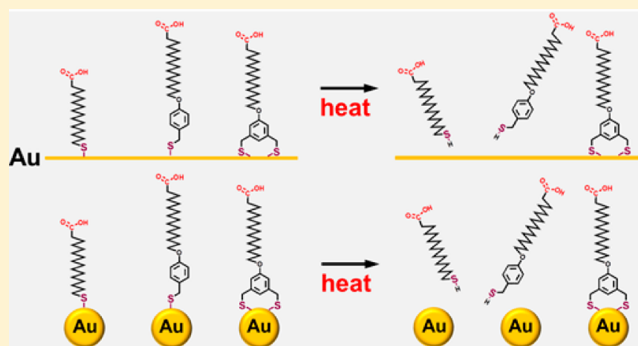
Robust Carboxylic Acid-Terminated Organic Thin Films and Nanoparticle Protectants Generated from Bidentate Alkanethiols

Han Ju Lee, Andrew C. Jamison, Yuehua Yuan, Chien-Hung Li, Supachai Rittikulsittichai, Irene Rusakova, and T. Randall Lee*

Department of Chemistry and the Texas Center for Superconductivity, University of Houston, 4800 Calhoun Road, Houston, Texas 77204-5003, United States

Supporting Information

ABSTRACT: A new carboxylic acid-terminated alkanethiol having bidentate character, 16-(3,5-bis(mercaptomethyl)phenoxy)hexadecanoic acid (**BMPHA**), was designed as an adsorbate and protectant to form thermally stable carboxylic acid-terminated organic thin films on flat gold and nanoparticles, respectively. The structural features of the organic thin films derived from **BMPHA** were characterized by ellipsometry, X-ray photoelectron spectroscopy (XPS), and polarization modulation infrared reflection absorption spectroscopy (PM-IRRAS), and compared to those derived from mercaptohexadecanoic acid (**MHA**) and 16-(4-(mercaptomethyl)phenoxy)hexadecanoic acid (**MMPHA**). This study demonstrates that films derived from **BMPHA** are less densely packed than films derived from **MHA** and **MMPHA**. However, the results of solution-phase thermal desorption tests revealed that the carboxylic acid-terminated films generated from **BMPHA** exhibit an enhanced thermal stability compared to those generated from **MHA** and **MMPHA**. Furthermore, as a nanoparticle protectant, **BMPHA** can be used to stabilize large gold nanoparticles (~45 nm diameter) in solution, and **BMPHA**-protected gold nanoparticles exhibited a high thermal stability in solution thermolysis studies.



INTRODUCTION

The exploration of new adsorbates for the generation of organic thin films on flat gold and nanoparticles is vital to emerging applications in the fields of medicine, sensors, and electronics. Among the many systems found in the literature, carboxylic acid-functionalized thin film coatings have been intensely studied for use in biosensors,^{1,2} drug-delivery systems,^{3–5} switching devices,^{6,7} and optical components.⁸ The broad interest in films bearing this fundamental functional group is due, in part, to the remarkable versatility of surfaces modified with carboxylic acid terminal groups. For example, carboxylic acids can readily be converted to esters and amides. Moreover, upon exposure to basic conditions, surface bound carboxylic acids can form ionic bonds with the positively charged terminus of an appropriate surfactant. Additionally, hydrogen bonds can be used to produce complex interactions between the terminal groups and ambient molecules bearing polar moieties. Despite the fact that hydrogen bonds (~21 kJ/mol) are weaker than covalent and ionic bonds, they clearly play important roles in a variety of phenomena (e.g., protein folding).⁹

The self-assembly of alkanethiol molecules is a simple and useful method to form organic thin films on metal surfaces and to functionalize metal nanoparticles. Self-assembled monolayers (SAMs) on gold can be easily prepared under ambient conditions and without complicated equipment such as

ultrahigh vacuum systems.¹⁰ SAMs can be generated on both curved surfaces as well as flat interfaces. In addition, control of interfacial properties such as wettability and friction can be readily achieved by changing the chemical nature of the adsorbates^{11–13} or by applying an electrical bias.¹⁴ However, organic thin films and protection layers for nanoparticles derived from alkanethiols are unstable under certain conditions, such as exposure to excess heat,^{15,16} UV light,^{17,18} and harsh chemicals.^{19,20} The lack of stability under these conditions limits the use of SAMs in many advanced applications.

Over the past 20 years, several strategies have been introduced to increase the stability of SAMs. In 1997, Kim et al. introduced photopolymerizable diacetylene groups into acid-terminated alkanethiols for enhancing the thermal and chemical stability of the fully formed SAM.²¹ Once cross-linked by UV treatment, the organic thin films survived exposure to 200 °C for 1 h and in hot basic solution for an extended time. The difficulties associated with their synthesis, handling, and manipulation, however, limited the widespread use of this strategy.

Received: May 6, 2013

Revised: July 10, 2013

Published: July 15, 2013

Several research groups explored an alternative method of enhancing the stability of SAMs by utilizing the intermolecular π - π interactions of aromatic rings. Sabatani et al. successfully improved the stability of SAMs on flat gold by increasing the number of aromatic rings in the system.²² However, the loss of conformational mobility for these highly conjugated adsorbates can create problems for their use in nanoparticle systems.²³ Tao et al. explored the use of a single aromatic ring near the gold surface²⁴ and examined the influence of the number of methylene units between the aromatic ring and the sulfur headgroup on the durability of SAMs through electrochemical measurements. These studies found that the monolayers generated from the phenyl-incorporating thiols with a single methylene spacer were better ordered than those derived from adsorbates with thiols directly attached to the aromatic ring.

Many research groups have also examined custom-designed alkanethiol adsorbates having multiple binding sites that generate organic thin films with enhanced thermal stability.^{25–30} In most cases, these multidentate alkanethiols readily generate SAMs on both flat or curved gold surfaces at room temperature and show an enhanced ability to withstand exposure to elevated temperatures in thermal desorption studies. The driving force of their stability is the chelate effect, which is the entropically favored binding of a multidentate adsorbate when compared to an equivalent number of analogous monodentate ligands.^{31,32}

With the aforementioned results in mind, we designed, synthesized, and studied a new carboxylic acid-terminated alkanethiol, 16-[3,5-bis(mercaptomethyl)phenoxy]hexadecanoic acid (**BMPHA**), in an effort toward the generation of highly stable carboxylic acid-terminated organic thin films. To provide a more complete analysis of the effectiveness of this class of adsorbate, we prepared a control system having an aromatic moiety within a monodentate analogue, 16-[4-(mercaptomethyl)phenoxy]hexadecanoic acid (**MMPHA**), and compared SAMs formed from both of these adsorbates against SAMs formed from the commonly used monothiol 16-mercaptohexadecanoic acid (**MHA**) (see Figure 1). Herein, we explore carboxylic acid-functionalized organic

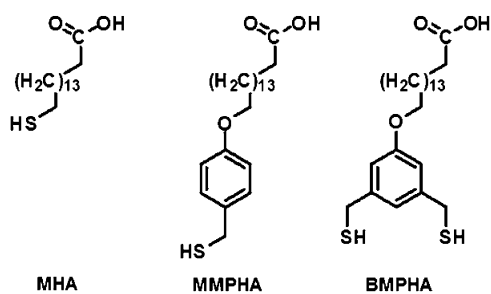


Figure 1. Structures of the carboxylic acid-terminated alkanethiols studied.

thin films prepared from **BMPHA**, **MMPHA**, **MHA**, and an octadecanethiol (**C18SH**) standard on evaporated “flat” gold and gold nanoparticles utilizing analytical methods that include ellipsometry, X-ray photoelectron spectroscopy (XPS), polarization modulation infrared reflection absorption spectroscopy (PM-IRRAS), and UV–vis spectroscopy. Furthermore, we evaluated the thermal stability of each of these systems to estimate their potential as scaffolds for the development of new materials and device architectures.

EXPERIMENTAL SECTION

Materials. ω -Hexadecalactone, dicyclohexylcarbodiimide (DCC), 4-(*N,N*-dimethyl-amino)pyridine (DMAP), lithium aluminum hydride (LiAlH_4), dimethyl 5-hydroxyisophthalate, 4-(hydroxymethyl)phenol, potassium carbonate (K_2CO_3), methanesulfonyl chloride (MsCl), triethylamine (Et_3N), potassium thioacetate, and octadecanethiol (**C18SH**) were purchased from Sigma-Aldrich and used as received. Tetrahydrofuran (THF), methanol (MeOH), dichloromethane (CH_2Cl_2), and chloroform (CHCl_3) were purchased from Sigma-Aldrich. Hexanes, ethyl acetate (EtOAc), and acetone were purchased from Mallinckrodt Chemicals. Anhydrous ethanol (EtOH) was purchased from Decon Lab, Inc. Distilling over calcium hydride gave dry tetrahydrofuran and dichloromethane. Water was purified to a resistance of 18 M Ω by use of an Academic Milli-Q Water System (Millipore Corporation) and filtered through a 0.22 μm membrane filter before use. Silica gel for column chromatography was obtained from Sorbent Technologies. Flat gold substrates were prepared by the thermal evaporation of gold (~ 1000 Å) onto chromium-coated (~ 100 Å) Si wafers under ultrahigh vacuum. The gold-coated wafers were cut into slides (1×4 cm²), rinsed with ethanol, and dried with ultrapure nitrogen before film formation. Citrate-stabilized gold nanoparticles (AuNPs) were synthesized by the reduction of HAuCl_4 with trisodium citrate according to literature procedures.³³ The average diameters of the gold nanoparticles used in this study were 25 and 45 nm as determined by SEM and/or TEM.

Preparation of Carboxylic Acid-Terminated Alkanethiols.

Detailed synthetic procedures for the synthesis and characterization of **MHA**, **MMPHA**, and **BMPHA** are provided in the Supporting Information.

Preparation of Carboxylic Acid-Functionalized Organic Thin Films on Flat Gold Surfaces. Organic thin films were prepared by immersing slides (1×4 cm²) of freshly prepared gold-coated silicon wafers in ethanolic solutions containing the appropriate carboxylic acid-terminated alkanethiols at 1 mM concentration. The glass vials containing the solutions were previously cleaned with piranha solution (3:1 mixture of concentrated H_2SO_4 /30 wt % H_2O_2) and rinsed thoroughly with copious amounts of deionized water and finally with ethanol. **Caution: Piranha solution is highly corrosive, should never be stored, and should be handled with extreme caution.** We also prepared SAMs using normal octadecanethiol (**C18SH**) as a reference, since octadecanethiol provides well-defined organic thin films on flat gold surfaces. All slides were incubated for 48 h, rinsed thoroughly with deionized water, THF, and ethanol, and then dried with a gentle stream of ultrapure nitrogen before analysis.

Characterization of Carboxylic Acid-Functionalized Organic Thin Films on Flat Gold Surfaces. **Ellipsometric Film Thickness Measurements.** The thicknesses of the organic thin films were evaluated using a Rudolph Research Auto EL III ellipsometer operating with a He–Ne laser (632.8 nm) at a fixed angle of incidence (70°) from the surface normal. A refractive index of 1.45 was assumed for all of the measurements. Values were taken from three different regions on at least two slides for each adsorbate. The reported values represent the averages of at least six data points (reproducibility within ± 2 Å).

Polarization Modulation Infrared Reflection Absorption Spectroscopy (PM-IRRAS) Measurements. Surface IR spectra were obtained with a Nicolet NEXUS 670 FT-IR spectrophotometer equipped with a liquid nitrogen-cooled mercury–cadmium–telluride (MCT) detector and Hinds Instrument PEM 90 photoelastic modulator operating at 37 kHz. The p-polarized light was reflected from the sample at an angle of incidence of 80° with respect to the surface normal. The spectra were collected over 128 scans at a spectral resolution of 2 cm⁻¹.

X-ray Photoelectron Spectroscopy (XPS) Measurements. A PHI 5700 X-ray photoelectron spectrometer equipped with a monochromatic Al $K\alpha$ X-ray source ($h\nu = 1486.7$ eV) incident at 90° relative to the axis of a hemispherical energy analyzer was used to obtain X-ray photoelectron spectra of freshly prepared samples. The spectrometer was configured to operate at high resolution with a pass energy of 23.5 eV, a photoelectron takeoff angle of 45° from the

surface, and an analyzer spot diameter of 2 mm. Spectra were collected at room temperature and at a base pressure of 2×10^{-8} Torr. The binding energies were referenced to that of the Au 4f_{7/2} peak at 84.0 eV.

Solution-Phase Desorption of Carboxylic Acid-Functionalized Organic Thin Films from Flat Gold Surfaces. According to a previously developed analytical method,^{15,34} the relative ellipsometric thicknesses of the films were used to determine the fraction of SAMs remaining on the surface. Organic thin films on gold slides were heated in unstirred solutions of either decalin or a mixture of deionized water and ethanol (water:ethanol = 2:1) at 90 °C as a function of time, followed by rinsing with deionized water, THF, and ethanol and drying with ultrapure nitrogen. The ellipsometric thicknesses of the sample were then immediately recorded.

Preparation of Carboxylic Acid-Functionalized Gold Nanoparticles. The carboxylic acid-functionalized gold nanoparticles were prepared by ligand exchange between carboxylic acid-terminated alkanethiols and citrate. A suspension of AuNPs in 20 mL of phosphate buffer (10 mM, pH 7.0, with 1.0 mg/mL Tween 20) was purged of oxygen by bubbling nitrogen gas through the suspension for 30 min. Then, the ethanolic solution of the appropriate carboxylic acid-terminated alkanethiols (0.5 mM, 10 mL) was introduced via syringe into the vials containing the AuNP suspension, and the final mixture was stirred for 48 h under an atmosphere of nitrogen. To remove excess carboxylic acid-terminated alkanethiol and Tween 20, the final mixture was washed twice (using centrifugation) with a mixture of phosphate buffer (pH 7.0, 10 mM) and ethanol (a 2:1 ratio of phosphate buffer:ethanol) and finally dispersed in a mixture of phosphate buffer (pH 7.0, 10 mM) and ethanol for testing. The stability of these carboxylic acid-terminated gold nanoparticles is influenced by the pH of the dispersion medium; therefore, pH 7.0 phosphate buffer was used for retaining a consistent carboxylic acid/carboxylate ion ratio during testing.^{35,36}

Solution Thermolysis of Carboxylic Acid-Functionalized Gold Nanoparticles. To evaluate the thermal stability of gold nanoparticles coated with MHA, MMPHA, and BMPHA, the optical properties of the carboxylic acid-functionalized gold nanoparticles as a function of thermal treatment in a mixture of phosphate buffer (10 mM, pH 7.0) and ethanol (phosphate buffer:ethanol = 2:1) at 90 °C were monitored by UV–visible spectroscopy²⁸ over the range 300–1000 nm using a Cary 50 scan UV–visible optical spectrometer (Varian) with Cary Win UV software. UV–visible spectra were recorded at room temperature by placing 3 mL aliquots of the samples in a quartz cell having a 1 cm optical path length.

Analysis of Carboxylic Acid-Functionalized Gold Nanoparticles by TEM. We analyzed the gold nanoparticles both before and after thermolysis by using a JEOL 2000 FX microscope equipped with an energy dispersive spectrometer operated at 200 kV. The samples for the TEM analyses were prepared by placing a drop of the colloidal solution from a pipet onto a TEM copper grid coated with an amorphous holey carbon film and then allowing the samples to dry in air.

RESULTS AND DISCUSSION

Characterization of Carboxylic Acid Functionalization Organic Thin Films on Flat Gold. For the SAMs generated on evaporated “flat” gold, we characterized the organic thin films derived from C18SH, MHA, MMPHA, and BMPHA using ellipsometry, XPS, and PM-IRRAS.

Measurements of Film Thickness. Table 1 shows the ellipsometric thicknesses of the SAMs generated from C18SH, MHA, MMPHA, and BMPHA and a comparison with those of the same or similar absorbates evaluated in previous studies.^{15,24} Within experimental uncertainty (± 2 Å), the ellipsometric thicknesses obtained in this study correspond well with values for the same or analogous SAM systems found in the literature.^{15,24} However, a detailed evaluation of the thickness of the SAM derived from BMPHA is warranted.

Table 1. Ellipsometric Thickness Measurements versus Previously Reported Thicknesses for Organic Thin Films Generated from C18SH, MHA, MMPHA, and BMPHA

absorbate	ellipsometric thickness ^a (Å)	reference thickness (Å)
C18SH	23	22 ¹⁵
MHA	21	21 ¹⁵
MMPHA	27	26 ^b
BMPHA	20	— ^c

^aThe reproducibilities of the ellipsometric thicknesses were within ± 2 Å. ^bEllipsometric thickness of [4,4'-(hexadecyloxy)phenyl] methanethiol.²⁴ ^cNo previous report.

Both MMPHA and BMPHA possess aromatic moieties along their backbones, and they are similar in molecular composition and chain length. Nevertheless, the ellipsometric thickness of the film generated from BMPHA is ~ 7 Å lower than that of the film generated from MMPHA (see Table 1). With two sulfur headgroups, BMPHA occupies more space on the surface of gold surfaces than does MMPHA.³⁷ Accordingly, the distance between BMPHA molecules on the surface must be greater, and the aliphatic chains of BMPHA are more tilted from the surface normal than those of MMPHA to optimize van der Waals interactions between the aliphatic chains. As a consequence, the SAM derived from BMPHA exhibits a smaller ellipsometric thickness than the SAM derived from MMPHA.

XPS Data Analysis. XPS can provide three aspects of important information in SAM studies: the nature of the bonds between the headgroups of the absorbates and substrates, the atomic composition of the organic thin films, and the relative packing densities of these films.^{38,39} Figure 2a shows the Au 4f region of the spectra obtained for all of the SAMs examined in this study; the spectra are all similar and otherwise unremarkable. Figure 2b shows that the binding energies for S 2p appearing at ~ 162 – 163.2 eV indicate bound thiolate for all of the adsorbates.⁴⁰ For these films, unbound thiol or disulfides (~ 164 – 166 eV) and oxidized sulfur (~ 169 eV) were not detected.^{41,42} These data are therefore consistent with a model in which all of the sulfur atoms are fully bound as thiolate to the surface of gold. To be more specific, the XPS data indicate that BMPHA is adsorbed onto the surface of gold via both sulfur headgroups simultaneously.

The XPS spectra highlighting the C 1s binding energy for the SAMs in Figure 2c exhibit three noteworthy results. First, the binding energies of the carboxylic acid carbon (around 289 eV) are detected only for the SAMs derived from MHA, MMPHA, and BMPHA.⁴³ Second, the peaks for the SAMs derived from MMPHA and BMPHA (at about 285 eV) are slightly broader than those for the SAMs derived from C18SH and MHA due to the overlapping of the peaks of the methylene carbons with those of the carbon atoms of the aromatic rings in the former.⁴⁴ Finally, the binding energies of the methylene carbons and the carbons of the aromatic ring of the BMPHA SAMs are shifted slightly lower than those of the other SAMs (~ 0.1 eV), which can be attributed to the fact that the positive charges generated by photoelectrons leaving loosely packed SAMs are more easily discharged than those in densely packed SAMs.^{45,46} This result supports a model in which the alkyl chains of the BMPHA SAMs are less densely packed than those of the other SAMs.

To obtain quantitative packing densities for the SAMs in this study, we used the areas of the peaks of the bands associated with the S 2p and Au 4f binding energies to derive sulfur-to-

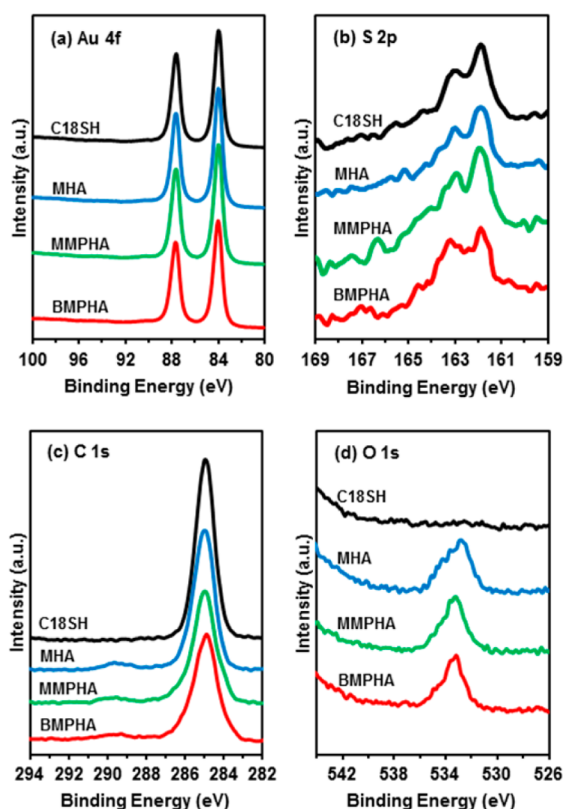


Figure 2. XPS spectra of the (a) Au 4f, (b) S 2p, (c) C 1s, and (d) O 1s spectral regions of the films derived from C18SH, MHA, MMPHA, and BMPHA.

gold (S/Au) ratios as described previously.⁴⁷ Assuming that the packing density of the C18SH film is 100%, we determined that the relative packing densities of the alkyl chains of the SAMs derived from MHA, MMPHA, and BMPHA films are 88, 75, and 45%, respectively (see Table 2). This quantitative analysis

Table 2. Relative Packing Densities for Organic Thin Films Derived from C18SH, MHA, MMPHA, and BMPHA

adsorbate	XPS peak area			relative packing density (%)
	Au 4f	S 2p	S/Au	
C18SH	93.98	6.02	0.064	100
MHA	94.69	5.31	0.056	88
MMPHA	95.44	4.59	0.048	75
BMPHA	94.44	5.56	0.029 ^a	45

^aTo compare with monodentate adsorbates, the S/Au ratio for BMPHA was divided by a factor of 2.

not only indicates that the BMPHA films have the lowest packing density, as was demonstrated with the XPS spectra of the C 1s binding energies, but can also be used to predict the relative conformational order or “crystallinity” of these monolayer films: C18SH > MHA > MMPHA > BMPHA.

PM-IRRAS Spectra. In organic thin film studies, surface infrared spectroscopy provides useful information such as characteristic peaks for functional groups and unique spectral trends for alkyl chain conformations.⁴⁸ With regard to the latter, the band position of the antisymmetric methylene C–H stretching vibration ($\nu_a^{\text{CH}_2}$) obtained from polarization modulation infrared reflection absorption spectroscopy (PM-IRRAS) can be used to evaluate the degree of order of organic

thin films.^{49,50} For example, $\nu_a^{\text{CH}_2}$ for a well-ordered heptadecanethiolate SAM appears at $\sim 2919 \text{ cm}^{-1}$, while that of the corresponding disordered film generated via partial thermal desorption appears at $\sim 2924 \text{ cm}^{-1}$.⁵¹ Figure 3 shows

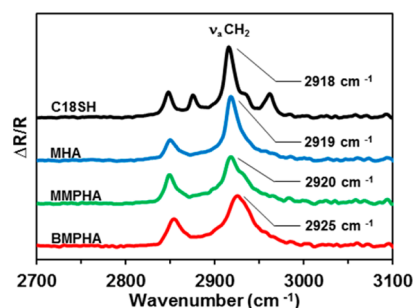


Figure 3. PM-IRRAS spectra of the C–H stretching region for the films generated from C18SH, MHA, MMPHA, and BMPHA.

that the band positions for $\nu_a^{\text{CH}_2}$ for SAMs generated from C18SH, MHA, MMPHA, and BMPHA are 2918, 2919, 2920, and 2925 cm^{-1} , respectively. These results indicate that the relative conformational order of these films is C18SH > MHA > MMPHA \gg BMPHA. These results are consistent with the relative packing densities obtained from XPS (vide supra). Apparently, the enhanced steric bulk of the BMPHA headgroup exerts a marked deleterious effect on the ordering of the resultant SAMs. Prior research using infrared spectroscopy that compared the conformational order of alkanethiolate SAMs on flat gold and on unsolvated AuNPs demonstrated that the ordering of the adsorbates on the two different surfaces was indistinguishable.⁵² Because of this prior work, we believe the relative packing densities of the alkyl chains of the adsorbates on the AuNP surfaces should be in accord with the relative packing densities for these SAMs on the “flat” gold surfaces.

Thermal Stability of the SAMs on Evaporated “Flat” Gold. To evaluate the thermal stability of the monolayer films generated from C18SH, MHA, MMPHA, and BMPHA, we carried out a series of solution-phase thermal desorption studies. In an initial set of experiments, we used ellipsometric thickness measurements to determine the average amount of adsorbate remaining after prolonged heating at 90 °C in a large excess of the nonpolar solvent decalin (decahydronaphthalene). Figure 4a highlights the remarkable difference between the films derived from BMPHA and those derived from the other adsorbates: while more than 80% of the BMPHA species remained on the surface after 12 h of heating, less than 40% of the adsorbates in the other SAMs remained under the same conditions. These results can be interpreted to indicate that the SAMs derived from BMPHA are markedly more stable than the SAMs derived from C18SH, MHA, and MMPHA.

To examine the influence of solvent (and adsorbate solubility) on the thermal stability, we performed analogous desorption experiments using the polar protic mixture of water and ethanol (2:1, v:v, respectively). When using this mixture as the desorption medium, the SAMs derived from BMPHA were still found to be the most stable (Figure 4b), but the differences between BMPHA SAMs and the other SAMs were less pronounced. As a whole, these results demonstrate that the SAMs derived from BMPHA are the most stable of all SAMs examined here; moreover, we can conclude that the bidentate headgroup is responsible for the enhanced stability, dominating the stabilization afforded by interchain packing effects.^{28,53}

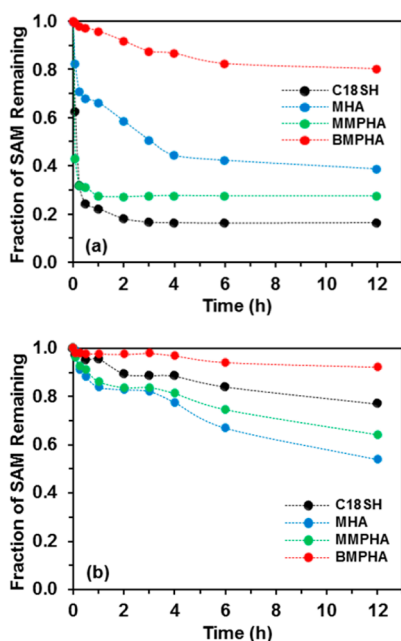


Figure 4. Solution-phase thermal desorption profiles of the indicated SAMs in (a) decalin and (b) a mixture of water and ethanol (water:ethanol = 2:1, v:v, respectively) at 90 °C.

Thermal Stability of SAM-Functionalized Gold Nanoparticles. As demonstrated in previous reports,^{35,36} the stability of gold nanoparticles dispersed in solvents can be estimated by UV–visible spectroscopy. For such studies, the particle size, stabilizer, and surrounding medium each have an influence on the surface plasmon resonance (SPR) bands for gold nanoparticles.⁵⁴ Furthermore, in cases where the gold nanoparticles aggregate and ultimately precipitate, red-shifting, broadening, and ultimately reduction of the intensity of the SPR bands are commonly observed.⁵⁵

In the present investigation, Figure 5a shows that, for small gold nanoparticles (25 nm) dispersed in a mixture of phosphate

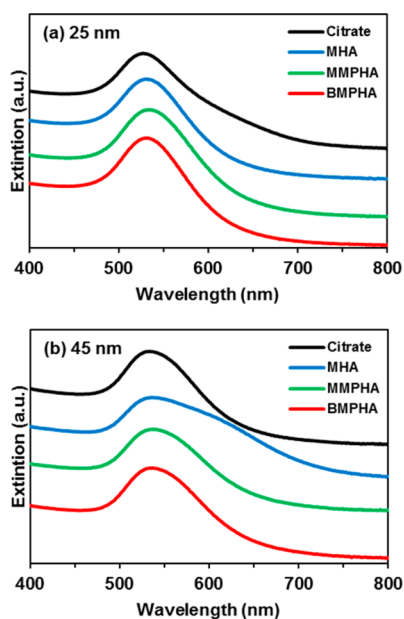


Figure 5. Visible spectra of (a) small and (b) large gold nanoparticles functionalized with citrate, MHA, MMPHA, and BMPHA.

buffer (10 mM, pH 7.0) and ethanol (2:1, v:v, respectively), there are no significant differences between the SPR bands of nanoparticles stabilized with MHA, MMPHA, BMPHA, and citrate. In contrast, noticeable differences in the SPR spectra of large gold nanoparticles (45 nm) are observed with the same set of adsorbates (see Figure 5b). The SPR band of citrate-stabilized gold nanoparticles having a diameter of 45 nm dispersed in deionized water appears at 531 nm. In contrast, the SPR bands of gold nanoparticles modified with MHA, MMPHA, and BMPHA dispersed in the aforementioned mixed buffer solution appear at ~536 nm.⁵⁶ Additionally, substantial broadening is observed only for the SPR band of the MHA-coated gold nanoparticles. It is likely that the observed red-shifts of the SPR bands are related to changes in the dielectric constant associated with the combination of the stabilizer and solvent.^{35,36,54} On the other hand, the broadening of the SPR band for the MHA-coated gold nanoparticles is likely due to nanoparticle aggregation.^{35,36} On the basis of these considerations, we conclude that MHA is ineffective at stabilizing the larger (45 nm) gold nanoparticles under the experimental conditions employed.

To evaluate the thermal stability of the carboxylic acid-functionalized gold nanoparticles, we monitored the changes in the SPR spectra of the 45 nm gold nanoparticles coated with citrate, MHA, MMPHA, and BMPHA as a function of time. For this experiment, the nanoparticles were suspended in a mixture of phosphate buffer (10 mM, pH 7.0) and ethanol (2:1, v:v, respectively) and placed in a bath maintained at 90 °C. For the citrate-capped nanoparticles, Figure 6a shows that the SPR

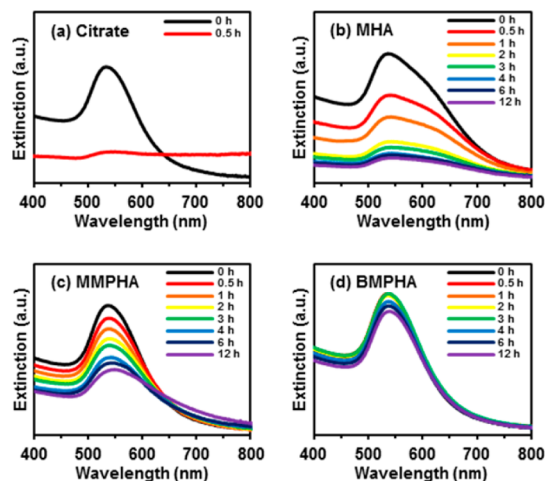


Figure 6. Time evolution of the visible extinction spectra in a solution of 10 mM phosphate buffer (pH 7.0) and ethanol (phosphate buffer:ethanol = 2:1, v:v) at 90 °C for 45 nm gold nanoparticles modified with (a) citrate, (b) MHA, (c) MMPHA, and (d) BMPHA.

band is almost nonexistent after 0.5 h of heating, suggesting rapid aggregation of the citrate-stabilized gold nanoparticles.⁵⁷ In contrast, parts b and c of Figure 6 show a relatively slow decrease in intensity and increase in broadening of the SPR peaks for the MHA- and MMPHA-modified gold nanoparticles, indicating that the aggregation of the nanoparticles is slower than that observed for the citrate-stabilized gold nanoparticles. Interestingly, Figure 6d of the BMPHA-coated gold nanoparticles shows a decrease in SPR intensity of only 12% after 12 h, indicating a substantially greater stabilizing influence of BMPHA compared to the other adsorbates.

Figure 7 provides additional evidence of the thermal stability of the **BMPHA**-coated gold nanoparticles at 90 °C in the

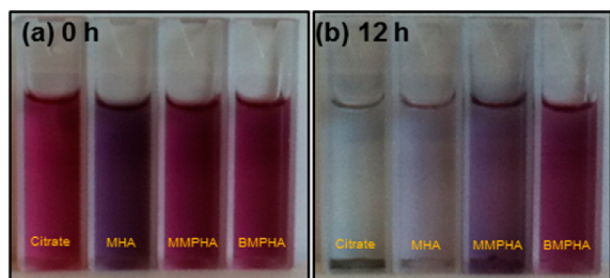


Figure 7. Photographs of dispersions of 45 nm gold nanoparticles in a solution of 10 mM phosphate buffer (pH 7.0) and ethanol (phosphate buffer:ethanol = 2:1, v:v) (a) before and (b) after thermolysis.

buffer:ethanol mixture. In particular, the solution of gold nanoparticles protected with **BMPHA** retains a red color after heating for 12 h, while the solutions of gold nanoparticles capped with citrate, **MHA**, and **MMPHA** turn either blue or clear due to aggregation and sedimentation, respectively.

We also collected TEM images of the carboxylic acid-functionalized gold nanoparticles before and after thermolysis (see Figure S5 in the Supporting Information). Even though AuNPs often aggregate as solvent is lost when preparing samples for analysis by TEM, we found systematic differences in the spacing of the nanoparticles in the TEM images. Before thermal treatment, only the **MHA**-coated AuNPs made contact with each other; the AuNPs functionalized with **MMPHA** and **BMPHA** had noticeable gaps between them. After thermolysis, the **MHA**-coated AuNPs clearly agglomerated, and the **MMPHA**-coated AuNPs made contact with each other. However, the **BMPHA**-coated AuNPs still had gaps between the particles. These results are consistent with the relative SAM/nanoparticle stabilities indicated by the optical data in Figures 6 and 7.

For a more quantitative evaluation of thermal stability, we utilized a modification of a prior method.²⁸ In Figure 8, the

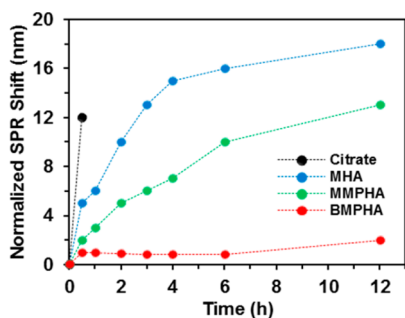


Figure 8. Profiles of the normalized SPR peak shifts for gold nanoparticles functionalized with citrate, **MHA**, **MMPHA**, and **BMPHA**.

normalized SPR shift is introduced as a semiempirical parameter. After 12 h, the position of the SPR band of the **BMPHA**-coated gold nanoparticles shifts by only 2 nm from the wavelength of the SPR band at 0 h, while those of **MHA**- and **MMPHA**-coated gold nanoparticles shift by 18 and 13 nm, respectively. As a whole, these profiles provide further evidence that the carboxylic acid-functionalized gold nanoparticles

protected with **BMPHA** are quantitatively more stable than those protected with the other adsorbates.

CONCLUSION

The new bidentate carboxylic acid-terminated alkanethiol, **BMPHA**, readily forms monolayers on flat and curved gold surfaces, with $\geq 80\%$ of the sulfur atoms bound to gold. Although the SAMs generated from **BMPHA** were less densely packed and less conformationally ordered than those generated from **MHA**, and **MMPHA**, the SAMs (and SAM-protected nanoparticles) derived from **BMPHA** are markedly more stable in both nonpolar and polar protic solvents when heated to 90 °C. The thermal stability of the **BMPHA** films can be attributed to the formation of multiple bonds between the adsorbates and the surface of gold via the “chelate effect”. We believe that our new bidentate carboxylic acid-terminated alkanethiol will offer a viable strategy for generating stable thin-film coatings with a pendant transformable functional group, leading to new applications for organic thin films as nanoscale coatings and nanoparticle protectants.

ASSOCIATED CONTENT

Supporting Information

Detailed descriptions of the synthetic procedures for the carboxylic acid-terminated alkanethiols along with the ^1H and ^{13}C NMR spectra of **BMPHA** and **MMPHA** and TEM images of the nanoparticles before and after thermolysis. This material is available free of charge via the Internet at <http://pubs.acs.org>.

AUTHOR INFORMATION

Corresponding Author

*E-mail: trlee@uh.edu.

Notes

The authors declare no competing financial interest.

ACKNOWLEDGMENTS

We thank the Robert A. Welch Foundation (Grant No. E-1320), the National Science Foundation (DMR-0906727), and the Texas Center for Superconductivity at the University of Houston for generous support.

REFERENCES

- (1) Patel, N.; Davies, M. C.; Hartshorne, M.; Heaton, R. J.; Roberts, C. J.; Tendler, S. J. B.; Williams, P. M. Immobilization of Protein Molecules onto Homogeneous and Mixed Carboxylate-Terminated Self-Assembled Monolayers. *Langmuir* **1997**, *13*, 6485–6490.
- (2) Frederix, F.; Bonroy, K.; Laureyn, W.; Reekmans, G.; Campitelli, A.; Dehaen, W.; Maes, G. Enhanced Performance of an Affinity Biosensor Interface Based on Mixed Self-Assembled Monolayers of Thiols on Gold. *Langmuir* **2003**, *19*, 4351–4357.
- (3) Giacomelli, C.; Schmidt, V.; Borsali, R. Specific Interactions Improve the Loading Capacity of Block Copolymer Micelles in Aqueous Media. *Langmuir* **2007**, *23*, 6947–6955.
- (4) Tian, L.; Hammond, P. T. Comb-Dendritic Block Copolymers as Tree-Shaped Macromolecular Amphiphiles for Nanoparticle Self-Assembly. *Chem. Mater.* **2006**, *18*, 3976–3984.
- (5) Keegan, M. K.; Falcone, J. L.; Leung, T. C.; Saltzman, W. M. Biodegradable Microspheres with Enhanced Capacity for Covalently Bound Surface Ligands. *Macromolecules* **2004**, *37*, 9779–9784.
- (6) Wu, Y.; Li, Y.; Ong, B. S. A Simple and Efficient Approach to a Printable Silver Conductor for Printed Electronics. *J. Am. Chem. Soc.* **2007**, *129*, 1862–1863.

- (7) Bao, Z.; Lovinger, A. J. Soluble Regioregular Polythiophene Derivatives as Semiconducting Materials for Field-Effect Transistors. *Chem. Mater.* **1999**, *11*, 2607–2612.
- (8) Kim, E.; Whitesides, G. M.; Lee, L. K.; Smith, S. P.; Prentiss, M. Fabrication of Arrays of Channel Waveguides by Self-Assembly Using Patterned Organic Monolayers as Templates. *Adv. Mater.* **1996**, *8*, 139–142.
- (9) Dill, K. A. Dominant Forces in Protein Folding. *Biochemistry* **1990**, *29*, 7133–7155.
- (10) Love, J. C.; Estroff, L. A.; Kriebel, J. K.; Nuzzo, R. G.; Whitesides, G. M. Self-Assembled Monolayers of Thiolates on Metals as a Form of Nanotechnology. *Chem. Rev.* **2005**, *105*, 1103–1169.
- (11) Ruths, M. Friction of Mixed and Single-Component Aromatic Monolayers in Contacts of Different Adhesive Strength. *J. Phys. Chem. B* **2006**, *110*, 2209–2218.
- (12) Zhang, H.-L.; Chen, M.; Li, H.-L. Study on Two-Component Matrix Formed by Coadsorption of Aromatic and Long Chain Mercaptans on Gold. *J. Phys. Chem. B* **2000**, *104*, 28–36.
- (13) Brewer, L. J.; Leggett, G. J. Chemical Force Microscopy of Mixed Self-Assembled Monolayers of Alkanethiols on Gold: Evidence for Phase Separation. *Langmuir* **2004**, *20*, 4109–4115.
- (14) Lahann, J.; Mitragotri, S.; Tran, T.-N.; Kaido, H.; Sundaram, J.; Choi, I. S.; Hoffer, S.; Somorjai, G. A.; Langer, R. A Reversibly Switching Surface. *Science* **2003**, *299*, 371–374.
- (15) Bain, C. D.; Troughton, E. B.; Tao, Y. T.; Evall, J.; Whitesides, G. M.; Nuzzo, R. G. Formation of Monolayer Films by the Spontaneous Assembly of Organic Thiols from Solution onto Gold. *J. Am. Chem. Soc.* **1989**, *111*, 321–340.
- (16) Bensebaa, F.; Ellis, T. H.; Badia, A.; Lennox, R. B. Probing the Different Phases of Self-Assembled Monolayers on Metal Surfaces: Temperature Dependence of the C-H Stretching Modes. *J. Vac. Sci. Technol., A* **1995**, *13*, 1331–1336.
- (17) Huang, J.; Hemminger, J. C. Photooxidation of Thiols in Self-Assembled Monolayers on Gold. *J. Am. Chem. Soc.* **1993**, *115*, 3342–3343.
- (18) Tam-Chang, S.-W.; Biebuyck, H. A.; Whitesides, G. M.; Jeon, N.; Nuzzo, R. G. Self-Assembled Monolayers on Gold Generated from Alkanethiols with the Structure $\text{RNHCOCH}_2\text{SH}$. *Langmuir* **1995**, *11*, 4371–4382.
- (19) Zamborini, F. P.; Crooks, R. M. In-Situ Electrochemical Scanning Tunneling Microscopy (ECSTM) Study of Cyanide-Induced Corrosion of Naked and Hexadecyl Mercaptan-Passivated Au(111). *Langmuir* **1997**, *13*, 122–126.
- (20) Nuzzo, R. G.; Fusco, F. A.; Allara, D. L. Spontaneously Organized Molecular Assemblies. 3. Preparation and Properties of Solution Adsorbed Monolayers of Organic Disulfides on Gold Surfaces. *J. Am. Chem. Soc.* **1987**, *109*, 2358–2368.
- (21) Kim, T.; Chan, K. C.; Crooks, R. M. Polymeric Self-Assembled Monolayers. 4. Chemical, Electrochemical, and Thermal Stability of ω -Functionalized Self-Assembled Diacetylenic and Polydiacetylenic Monolayers. *J. Am. Chem. Soc.* **1997**, *119*, 189–193.
- (22) Sabatani, E.; Cohen-Boulakia, J.; Bruening, M.; Rubinstein, I. Thioaromatic Monolayers on Gold: A New Family of Self-Assembling Monolayers. *Langmuir* **1993**, *9*, 2974–2981.
- (23) Tao, Y.-T.; Wu, C.-C.; Eu, J.-Y.; Lin, W.-L. Adsorption of 4-Biphenylmethanethiolate on Different-Sized Gold Nanoparticle Surface. *Langmuir* **2004**, *20*, 1922–1927.
- (24) Jang, S.; Park, J.; Shin, S.; Yoon, C.; Choi, B. K.; Gong, M.-S.; Joo, S.-W. Structure Evolution of Aromatic-Derivatized Thiol Monolayers on Evaporated Gold. *Langmuir* **1997**, *13*, 4018–4023.
- (25) Zhang, S.; Palkar, A.; Echegoyen, L. Selective Anion Sensing Based on Tetra-Amide Calix[6]arene Derivatives in Solution and Immobilized on Gold Surfaces via Self-Assembled Monolayers. *Langmuir* **2006**, *22*, 10732–10738.
- (26) Garg, N.; Lee, T. R. Self-Assembled Monolayers Based on Chelating Aromatic Dithiols on Gold. *Langmuir* **1998**, *14*, 3815–3819.
- (27) Zhang, S.; Leem, G.; Srisombat, L.; Lee, T. R. Rationally Designed Ligands That Inhibit the Aggregation of Large Gold Nanoparticles in Solution. *J. Am. Chem. Soc.* **2008**, *130*, 113–120.
- (28) Srisombat, L.; Zhang, S.; Lee, T. R. Thermal Stability of Mono-, Bis-, and Tris-Chelating Alkanethiol Films Assembled on Gold Nanoparticles and Evaporated “Flat” Gold. *Langmuir* **2010**, *26*, 41–46.
- (29) Perumal, S.; Hofmann, A.; Scholz, N.; Rühl, E.; Graf, C. Kinetics Study of the Binding of Multivalent Ligands on Size-Selected Gold Nanoparticles. *Langmuir* **2011**, *27*, 4456–4464.
- (30) Ge, D.; Wang, X.; Williams, K.; Levicky, R. Thermostable DNA Immobilization and Temperature Effects on Surface Hybridization. *Langmuir* **2012**, *28*, 8446–8455.
- (31) Chinwangso, P.; Jamison, A. C.; Lee, T. R. Multidentate Adsorbates for Self-Assembled Monolayer Films. *Acc. Chem. Res.* **2011**, *44*, 511–519.
- (32) Srisombat, L.; Jamison, A. C.; Lee, T. R. Stability: A Key Issue for Self-Assembled Monolayers as Thin-Film Coatings and Nanoparticle Protectants. *Colloids Surf., A* **2011**, *390*, 1–19.
- (33) Frens, G. Controlled Nucleation for the Regulation of the Particles Size in Monodisperse Gold Suspensions. *Nature* **1973**, *241*, 20–22.
- (34) Jennings, G. K.; Laibinis, P. E. Underpotentially Deposited Metal Layers of Silver Provide Enhanced Stability to Self-Assembled Alkanethiol Monolayers on Gold. *Langmuir* **1996**, *12*, 6173–6175.
- (35) Weisbecker, C. S.; Merritt, M. V.; Whitesides, G. M. Molecular Self-Assembly of Aliphatic Thiols on Gold Colloids. *Langmuir* **1996**, *12*, 3763–3772.
- (36) Mayya, K. S.; Patil, V.; Sastry, M. On the Stability of Carboxylic Acid Derivatized Gold Colloidal Particles: The Role of Colloidal Solution pH Studied by Optical Absorption Spectroscopy. *Langmuir* **1997**, *13*, 3944–3947.
- (37) Bruno, G.; Babudri, F.; Operamolla, A.; Bianco, G. V.; Losurdo, M.; Giangregorio, M. M.; Hassan Omar, O.; Mavelli, F.; Farinola, G. M.; Capezzuto, P.; Naso, F. Tailoring Density and Optical and Thermal Behavior of Gold Surfaces and Nanoparticles Exploiting Aromatic Dithiols. *Langmuir* **2010**, *26*, 8430–8440.
- (38) Lu, H. B.; Campbell, C. T.; Castner, D. G. Attachment of Functionalized Poly(ethylene glycol) Films to Gold Surfaces. *Langmuir* **2000**, *16*, 1711–1718.
- (39) Laibinis, P. E.; Whitesides, G. M.; Allara, D. L.; Tao, Y. T.; Parikh, A. N.; Nuzzo, R. G. Comparison of the Structures and Wetting Properties of Self-Assembled Monolayers of *n*-Alkanethiols on the Coinage Metal Surfaces, Cu, Ag, Au. *J. Am. Chem. Soc.* **1991**, *113*, 7152–7167.
- (40) Yang, Y. W.; Fan, L. J. High-Resolution XPS Study of Decanethiol on Au(111): Single Sulfur-Gold Bonding Interaction. *Langmuir* **2002**, *18*, 1157–1164.
- (41) Castner, D. G.; Hinds, K.; Grainger, D. W. X-ray Photoelectron Spectroscopy Sulfur 2p Study of Organic Thiol and Disulfide Binding Interactions with Gold Surfaces. *Langmuir* **1996**, *12*, 5083–5086.
- (42) Heeg, J.; Schubert, U.; Kuchenmeister, F. Mixed Self-Assembled Monolayers of Terminally Functionalized Thiols at Gold Surfaces Characterized by Angle Resolved X-ray Photoelectron Spectroscopy (ARXPS) Studies. *Fresenius' J. Anal. Chem.* **1999**, *365*, 272–276.
- (43) Stettner, J.; Frank, P.; Griesser, T.; Trimmel, G.; Schennach, R.; Gilli, E.; Winkler, A. A Study on the Formation and Thermal Stability of 11-MUA SAMs on Au(111)Mica and on Polycrystalline Gold Foils. *Langmuir* **2009**, *25*, 1427–1433.
- (44) Hallmann, L.; Bashir, A.; Strunskus, T.; Adelung, R.; Staemmler, V.; Woll, C.; Tuczek, F. Self-Assembled Monolayers of Benzylmercaptan and *p*-Cyanobenzylmercaptan on Au(111) Surfaces: Structural and Spectroscopic Characterization. *Langmuir* **2008**, *24*, 5726–5733.
- (45) Ishida, T.; Hara, M.; Kojima, I.; Tsuneda, S.; Nishida, N.; Sasabe, H.; Knoll, W. High Resolution X-ray Photoelectron Spectroscopy Measurements of Octadecanethiol Self-Assembled Monolayers on Au(111). *Langmuir* **1998**, *14*, 2092–2096.
- (46) Park, J.-S.; Vo, A. N.; Barriet, D.; Shon, Y.-S.; Lee, T. R. Systematic Control of the Packing Density of Self-Assembled Monolayers Using Bidentate and Tridentate Chelating Alkanethiols. *Langmuir* **2005**, *21*, 2902–2911.

(47) Rittikulsittichai, S.; Jamison, A. C.; Lee, T. R. Self-Assembled Monolayers Derived from Alkoxyphenylethanethiols Having One, Two, and Three Pendant Chains. *Langmuir* **2011**, *27*, 9920–9927.

(48) Perry, S. S.; Somorjai, G. A. Characterization of Organic Surfaces. *Anal. Chem.* **1994**, *66*, 403–415.

(49) Nuzzo, R. G.; Dubois, L. H.; Allara, D. L. Fundamental Studies of Microscopic Wetting on Organic Surfaces. I. Formation and Structural Characterization of a Self-Consistent Series of Polyfunctional Organic Monolayers. *J. Am. Chem. Soc.* **1990**, *112*, 558–569.

(50) Bensebaa, F.; Voicu, R.; Huron, L.; Ellis, T. H.; Kruus, H. Kinetics of Formation of Long-Chain *n*-Alkanethiolate Monolayers on Polycrystalline Gold. *Langmuir* **1997**, *13*, 5335–5340.

(51) Shon, Y.-S.; Lee, T. R. Desorption and Exchange of Self-Assembled Monolayers (SAMs) on Gold Generated from Chelating Alkanedithiols. *J. Phys. Chem. B* **2000**, *104*, 8192–8200.

(52) Porter, L. A.; Ji, D.; Westcott, S. L.; Graupe, M.; Czernuszewicz, R. S.; Halas, N. J.; Lee, T. R. Gold and Silver Nanoparticles Functionalized by the Adsorption of Dialkyl Disulfides. *Langmuir* **1998**, *14*, 7378–7386.

(53) Garg, N.; Carrasquillo-Molina, E.; Lee, T. R. Self-Assembled Monolayers Composed of Aromatic Thiols on Gold: Structural Characterization and Thermal Stability in Solution. *Langmuir* **2002**, *18*, 2717–2726.

(54) Underwood, S.; Mulvaney, P. Effect of the Solution Refractive Index on the Color of Gold Colloids. *Langmuir* **1994**, *10*, 3427–3430.

(55) Wiesner, J.; Wokaun, A. Anisotropic Gold Colloid. Preparation, Characterization, and Optical Properties. *Chem. Phys. Lett.* **1989**, *157*, 569–575.

(56) The SPR bands of citrate stabilized gold nanoparticles also shift to 533 nm due to the change of surrounding medium from distilled water to a mixture of phosphate buffer (10 mM, pH 7.0) and ethanol.

(57) Rouhana, L. L.; Jaber, J. A.; Schlenoff, J. B. Aggregation-Resistant Water-Soluble Gold Nanoparticles. *Langmuir* **2007**, *23*, 12799–12801.